Toward a Time-Scale Based Framework for ABR Traffic Management *

Tamer Dağ   Ioannis Stavrakakis
Electrical and Computer Engineering Department
409 Dana Research Building, 360 Huntington Avenue
Northeastern University, Boston, MA 02115
e-mail: ioannis@hilbert.cdsp.neu.edu

Abstract

This paper discusses a number of issues and possibilities for more effective ABR (Available Bit Rate) traffic management which arise from a careful consideration of various time scales present in an ATM networking environment. Since the ABR applications use the remaining resources after CBR (Constant Bit Rate) and VBR (Variable Bit Rate) applications have been accommodated, the ABR rate should be controlled through a feedback based flow control scheme to avoid excessive losses. It is well known that the increased propagation delay increases the amount of bandwidth mismatch which may induce cell losses. For this reason, the effectiveness of feedback based flow control schemes reduce with increased propagation delay. But, besides the propagation delay, some other system parameters (network, ABR and VBR time scales) may also have considerable effects on the feedback based flow control schemes. In this paper by considering a tractable analytical model, the impact of these time scales is considered. Also, a proactive feedback based flow control scheme which aims to reduce the amount of bandwidth mismatch by generating early feedbacks is introduced.

1 Introduction

The ABR service class is one of the the four service classes defined by the ATM Forum [1]. It is intended for non-real time applications which can tolerate delay by using the remaining bandwidth left from VBR and CBR applications. Since the bandwidth availability for the ABR service class is time-varying due to the fluctuations in the VBR and CBR traffic, a feedback based flow control should be applied to control the rates of the ABR traffic sources.

Two different approaches for the feedback based flow control were considered: The rate based flow control [2], [3], [4] and the credit based flow control [5], [6], [7]. An integration of both schemes was also considered [8].

The credit based flow control is implemented link by link and per virtual circuit (VC). Before transmitting any cell through the link, the sender associated with the VC receives credits for the

*This research is supported in part by the Advanced Research Project Agency under Grant F49620-93-1-0564 monitored by the Air Force Office of Scientific Research (AFOSR) and the National Science Foundation under Grant NCR-9628116.

VC from the receiver where the credit shows the amount of buffer space available at the receiver. The sender then can transmit any number of cells up to its credit balance to avoid cell losses.

In the rate based flow control, the sender is notified about congestion in the network with a feedback generated at the receiver or at any congested node. When the sender receives the feedback, it adjusts its rate according to the control scheme in effect.

Although the credit based flow control can handle both smooth and bursty traffic (while the rate based flow control may not be very effective for bursty traffic), it introduces an excessive amount of overhead and is expected to be very expensive for a wide area network. For such reasons, the more flexible rate based flow control was adopted by the ATM Forum. Several traffic control policies have been proposed for the rate based flow control such as the Explicit Forward Congestion Indication (EFCI) [9], Backward Explicit Congestion Notification (BECN) [10], Proportional Rate Control Algorithm (PRCA) [11], Explicit Rate Feedback (ERF) [12] and Enhanced Proportional Rate Control Algorithm (EPRCA) [13].

Under the flow control scheme described in this paper, the ABR traffic source is notified about the bandwidth availability, when the VBR/CBR source rate changes. Thus, at the instant of a VBR/CBR source rate change, a feedback is generated at the network access node and transmitted to the ABR source. In the rest of this paper, this flow control scheme will be referred as the non-proactive feedback based flow control (*NPF*) scheme.

Assume that the forward and backward propagation delays are equal to T_d and the VBR/CBR source rate changes at time t_1 as shown in Figure 1. Because of the propagation delay, the ABR source will learn about the change in bandwidth availability at time $t_1 + T_d$ and the adjusted rate from the ABR source will reach the network access node at time $t_1 + 2T_d$. Since the VBR rate change has occurred at time t_1, a bandwidth mismatch will occur for a roundtrip propagation delay of $2T_d$. During this interval as the link capacity is exceeded, cell losses may occur depending on the amount of buffering available. Since the amount of bandwidth mismatch depends on the propagation delay, increased propagation delay reduces the effectiveness of feedback based flow control schemes. The effects of increased propagation delay on the effectiveness of feedback based flow control schemes have been studied in past [14], [15], [16], [17]. But, in addition to the propagation delay, some other system parameters may have considerable effects on the feedback based flow control schemes. In this paper, the impact of these system parameters (network, VBR and ABR time scales) will be investigated.

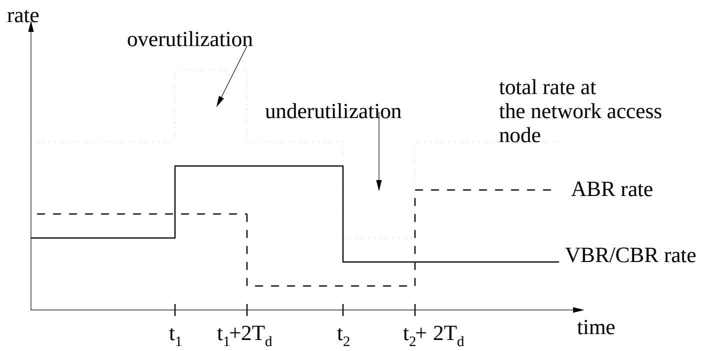

Figure 1: A bandwidth mismatch example under the NPF scheme

The network time scale is defined to be the transmission time of a cell (slot). As the network time scale decreases, the propagation delay increases. Thus, the decreased network time scale has a similar impact on the feedback based flow control schemes as the increased propagation delay.

The frequency of change of bandwidth availability also impact significantly the feedback based flow control schemes. If for a given time interval the number of VBR/CBR source rate changes increases, then the number of initiated bandwidth mismatch cycles will increase as well. Since increased number of bandwidth mismatch cycles will increase the number of overutilization periods, more cell losses will be induced and the effectiveness of the feedback based flow control schemes will reduce. Thus, the VBR time scale can be defined as the inverse of the frequency of VBR source rate changes or the average time over which VBR applications maintain a constant rate. The VBR time scale will demonstrate the above impact on the effectiveness of feedback based flow control schemes.

In addition to the network and VBR time scales, the cell transmission patterns of the ABR sources have substantial importance on the effectiveness of feedback based flow control schemes. It can be observed that between two ABR applications of the same rate, the one which transmits blocks of multiple cells every one of longer periods may utilize the resources better than the one which transmits one cell every one of shorter periods. The ABR time scale is therefore defined as the length of these periods and will reflect the effects of various transmission patterns on the feedback based flow control schemes.

Since losses may occur only because of the bandwidth mismatch, eliminating the bandwidth mismatch will reduce the losses to zero. Thus, when the bandwidth mismatch is eliminated, neither the network time scale nor the VBR time scale will have a negative impact on the effectiveness of feedback based flow control schemes. This can be possible if the exact time instants of the VBR source rate changes are known at the network access node and the feedbacks are generated a roundtrip propagation delay before the rate changes occur. Figure 2 illustrates the VBR and ABR source rates at the network access node under the early feedback transmission scheme. If the network access node knows that the VBR rate change will occur at time t_1, then it can generate the feedback for the ABR source at time $t_1 - 2T_d$. Since a roundtrip propagation delay is necessary for the adjusted ABR source rates to return back to the network access node, the adjusted ABR source rates will be at the network access node at time t_1 and the bandwidth mismatch will be completely eliminated. For some VBR applications such as the MPEG video applications, a fixed cell rate is maintained over well defined intervals. If the resource management cells carry information about the rate associated with the next such interval, then early feedback generation can be possible. If these intervals are randomly distributed, the network access node can estimate the time of the rate changes and generate the feedback according to its estimated rate change time. If a good estimator can be chosen, the amount of bandwidth mismatch can still be reduced (thus the ABR cell losses will also be reduced). In this paper, the briefly described feedback based flow control scheme which aims to decrease amount of bandwidth mismatch by generating early feedbacks will be referred as the proactive feedback based flow control (*PF*) scheme. Under the *PF* scheme the amount of bandwidth mismatch will be calculated and compared with the amount of bandwidth mismatch under the *NPF* scheme. Some simulation results will be presented to demonstrate the effectiveness of the *PF* scheme against the *NPF* schemes.

The remainder of this paper is organized as follows. In Section 2, the environment and the system used for this work is described. In Section 3, the ABR cell loss probability for the *NPF* scheme is derived. In Section 4, the *PF* scheme is introduced and a comparison between the

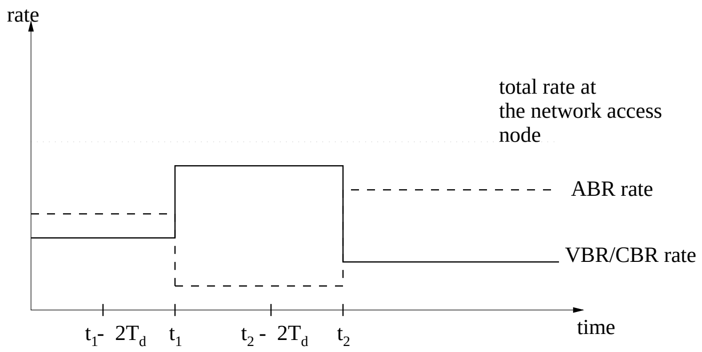

Figure 2: A bandwidth mismatch example under the PF scheme

NPF and *PF* schemes is made in terms of the amount of bandwidth mismatch occurring under both schemes. In Section 5, some numerical results are presented and the paper end with the conclusions made in Section 6.

2 Description of the System

In order to simplify the analysis and facilitate the understanding of the impact of various time scales, a transmission link shared by one VBR source and one ABR source will be considered where the ABR traffic source is away from the network access node (thus the propagation delay between the ABR source and the network access node is non-negligible). The distance between the VBR source and the network access node has no importance since no control is applied on the VBR source.

The network access node is assumed to have a buffer of capacity C to temporarily store the ABR source cells when the transmission link attends to the VBR traffic. A queuing model of the network access node is shown in Figure 3. It is assumed that both traffic sources may transmit at most one cell per slot, thus a buffer with capacity 1 will be sufficient for the VBR queue.

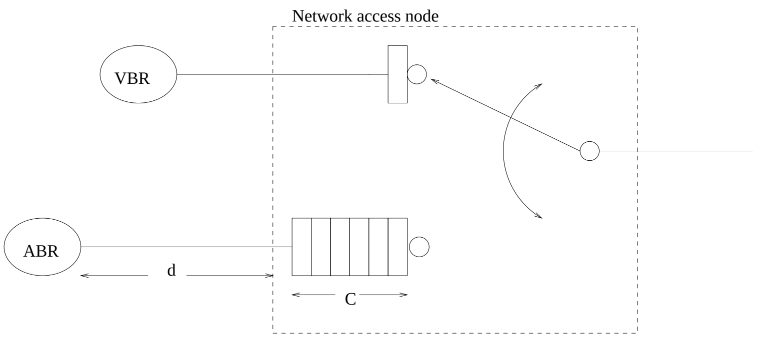

Figure 3: A queuing model of the network access node

2.1 The ABR Traffic Source

The maximum allowable ABR source rate can be calculated from the current VBR source rate. If the latter is equal to r_v, then the maximum allowable ABR source rate will be $1 - r_v - \epsilon$. Here, ϵ is a small positive number determined by the desirable load at the network access node.

To maintain its maximum allowable rate, the ABR source can transmit one cell per T_k slots where $T_k = \lceil \frac{1}{1-r_v-\epsilon} \rceil$ and $\lceil () \rceil$ denotes the smallest integer larger than (). In this paper, T_k will be denoted as the *fundamental ABR subframe*. The same rate can also be achieved, if the ABR source transmits B_k cells per subframe of length $B_k T_k$, that is, if the ABR source employs a B_k-order subframe where $B_k \in N$.

Thus, if $B_k = 1$, then the ABR source will employ the fundamental subframe T_k to transmit at a rate equal to $1/T_k$. If $B_k > 1$, the ABR source will employ a B_k-order subframe to transmit at the same rate equal to $1/T_k$. Figure 4 shows examples of ABR cell transmission employing fundamental or higher-order subframes.

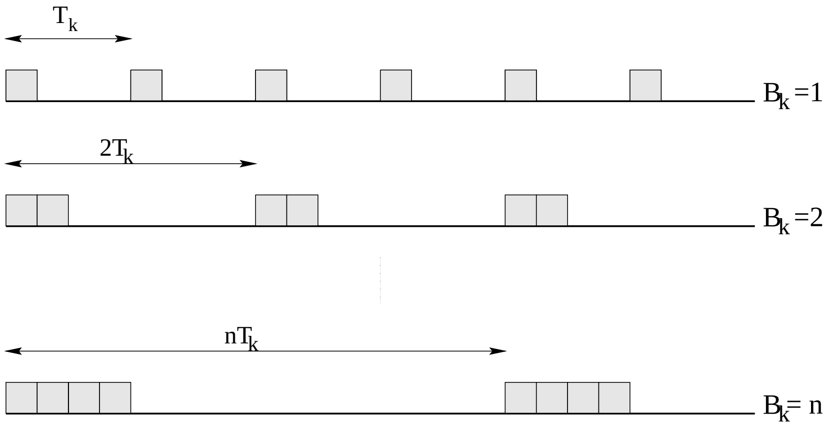

Figure 4: The ABR traffic subframes

Let $TC(B_k, B_k T_k)$ denote a transmission control policy according to which the ABR source transmits a batch with size B_k at the beginning of a subframe of length $B_k T_k$. Let $\overline{TC}(T_k) = \{TC(B_k, B_k T_k), B_k \geq 1\}$ denote the class of all $TC(B_k, B_k T_k)$ policies which implement the same transmission rate of $1/T_k$. This class of policies is characterized by the fundamental subframe of length T_k.

Let t_k denote the beginning time instant of the k^{th} subframe. At t_k, a fundamental subframe T_k (and ABR rate) will be determined based on the current VBR rate. Any policy in $\overline{TC}(T_k)$ can be selected for the implementation of the ABR source rate of $1/T_k$. As long as the VBR rate remains constant, the same policy will be employed. That is, if $T_{k+1} = T_k$ then $B_{k+1} = B_k$ and $TC(B_k, T_k) \equiv TC(B_{k+1}, T_{k+1})$. However, if a VBR source rate change occurs, then the network access node calculates the new ABR fundamental subframe T_{k+1} and any policy in $\overline{TC}(T_{k+1})$ can be selected.

The ABR time scale is defined as the length of the B_k-order subframe used to transmit ABR cells and one of the objectives of this paper is to evaluate the impact of ABR time scales on the effectiveness of feedback based flow control schemes. It is expected that the ABR time scale will have considerable importance.

2.2 The VBR Traffic Source

In this paper, it will be assumed that the activity level of the VBR source changes at subframe boundaries for analysis tractability. Let $\{S_k\}_{k\geq 1}$ be a 2-state underlying Markov chain with state space $\overline{S} = \{0, 1\}$ embedded at subframe boundaries $\{t_k\}_{k\geq 1}$ of length $B_k T_k$, where $B_k T_k$ is determined by the perceived remaining capacity as shown in the previous subsection.

Let $r_v(s_k)$ denote the rate of the VBR source at the k^{th} subframe where $r_v(1) > r_v(0)$. The VBR cell arrival process is modeled as a Markov Modulated Bernoulli process. The probability of transmitting 1 (0) cell in a slot of the k^{th} subframe is $r_v(s_k)$ $(1 - r_v(s_k))$. Therefore, the number of VBR cell arrivals during a slot of the k^{th} subframe, $A(s_k)$, is given by,

$$A(s_k) = \begin{cases} 1 & \text{with probability } r_v(s_k) \\ 0 & \text{with probability } 1 - r_v(s_k) \end{cases}$$

Let $p_s(s_k)$ denote the probability that S_k changes at the end of the k^{th} subframe at the beginning of which it was in state s_k. $p_s(s_k)$ will reflect the average time over which VBR applications maintain a constant rate (or VBR time scale). It is expected that the increased VBR time scale will increase the effectiveness of the feedback based flow control schemes.

3 Analysis of the System

In this section, a numerical approach is developed for the evaluation of the loss performance of the queuing model of the system shown in Figure 3. Since, the VBR traffic is provided prioritized service and the maximum number of VBR cell arrivals per slot is 1, no VBR cell losses will occur. For this reason, the analysis will focus on the evaluation of ABR cell losses. After deriving the ABR cell loss probability, the impact of time scales considered in this paper will be evaluated in terms of the ABR cell loss probability.

Let $\{S_k, Q_k\}_{k\geq 1}$ be a 2-dimensional process embedded at subframe boundaries $\{t_k\}_{k\geq 1}$ where Q_k is a random variable describing the buffer occupancy at t_k and $0 \leq q_k \leq C$. S_k completely determines the VBR arrival process. But, in order to determine the ABR arrival process at the network access node, the network access node needs to know the current VBR source rate $(r_v(s_k))$ and whether the current ABR rate is based on the most recent feedback sent by the network access node or not (in other words whether the feedback's impact is not pending or pending). Therefore, another random variable which describes the status of the impact of the feedback can be introduced. Let J_k be an indicator function which assumes the value of 1, if the impact of a feedback carrying a VBR source rate change is pending. If the impact of the feedback is not pending, J_k assumes the value of 0.

With this information, the ABR source rate at the network access node can be completely determined and it is equal to $1 - r_v(s_k \oplus j_k) - \epsilon$ where $\oplus$ denotes the modulo 2 addition.

A Markov chain can be constructed to describe the evolution of the system under fixed and non-zero roundtrip propagation delays. But, a simplifying assumption is made by assuming that the roundtrip propagation delay is random and geometrically distributed with mean $\frac{1}{p_f}$, measured in terms of subframes.

Although it is possible that at any time, the impact of more than one feedbacks is pending, at most one pending feedback will be considered in order to simplify the analysis. This approximation will hold true if $max_{s_k}\{p_s(s_k)\} \ll p_f$; that is, if the VBR source time scale is much larger than the propagation delay.

Under the above assumptions, it is easy to establish that the stochastic process $\{S_k, J_k, Q_k\}$ embedded at subframe boundaries is a Markov chain with state space $\{(s_k, j_k, q_k) : 0 \leq s_k \leq 1, 0 \leq j_k \leq 1, 0 \leq q_k \leq C\}$.

Let $P(s_k j_k q_k; s_{k+1} j_{k+1} q_{k+1})$ be the probability that the Markov chain $\{S_k, J_k, Q_k\}$ moves from state (s_k, j_k, q_k) at time t_k, to state $(s_{k+1}, j_{k+1}, q_{k+1})$ at time t_{k+1}. From the description of the system model, it can be understood that (s_{k+1}, j_{k+1}) evolves independently from the queue occupancy q_k and thus $P(s_k j_k q_k; s_{k+1} j_{k+1} q_{k+1})$ can be expressed as,

$$P(s_k j_k q_k; s_{k+1} j_{k+1} q_{k+1}) = P(s_k j_k; s_{k+1} j_{k+1}) P(q_{k+1}/s_k j_k q_k).$$

In the above equation, $P(s_k j_k; s_{k+1} j_{k+1})$ denotes the probability of passing from state $(s_k j_k)$ to state $(s_{k+1} j_{k+1})$ (or the conditional probability of being at state $(s_{k+1} j_{k+1})$ given the current state $(s_k j_k)$) and $P(q_{k+1}/s_k j_k q_k)$ denotes the probability of being at queue occupancy q_{k+1} at the beginning of the next subframe given the current subframe parameters. The derivation of these probabilities are shown in detail in the Appendix.

After the calculation of the transition probabilities, the steady state probability distribution $\Pi(s_k, j_k, q_k)$ can be derived by solving the following matrix equations, $\Pi = \Pi P$ and $\sum_i \Pi_i = 1$ where each element of the P matrix show the transition probabilities.

The ABR cell loss probability can be calculated using the average number of cells lost and arrived in a subframe $\{S_k, J_k, Q_k\}_{k \geq 1}$ in state (s_k, j_k, q_k) and taking the expectation over all possible states. Let LP, $\overline{L}(s_k, j_k, q_k)$ and $\overline{M}(s_k, j_k, q_k)$ denote the ABR cell loss probability, the average number of cells lost in a subframe and the average number of cells arrived in a subframe, respectively. Thus,

$$\begin{aligned} LP &= E\{\frac{\overline{L}(s_k, j_k, q_k)}{\overline{M}(s_k, j_k, q_k)}\} \\ &= \sum_{s_k=0}^{1} \sum_{j_k=0}^{1} \sum_{q_k=0}^{C} \frac{\Pi(s_k, j_k, q_k)}{B_k + r_v(s_k) B_k T_k} \sum_{i=1}^{B_k} \sum_{l=0}^{C} \sum_{m=0}^{l-C+1} m P\{A(s_k) = C - l + m/q_k, s_k, j_k\} \\ &\times \; P\{q_{k,i-1} = l/q_{k,0} = q_k\} \end{aligned}$$

The derivation of the ABR cell loss probability, LP is also shown in detail in the Appendix.

4 An Attempt to Decrease Bandwidth Mismatch: Early Feedback Generation

In the previous section, the cell loss probability for the ABR source was derived in order to evaluate the impact of various time scales on the effectiveness of the feedback based flow control schemes. As indicated previously, the bandwidth mismatch is the reason for ABR cell losses and increased amount of bandwidth mismatch reduces the effectiveness of feedback based flow control schemes. In this section, the *PF* scheme which tries to reduce the bandwidth mismatch by generating early feedbacks will be described. Thus, under the *PF* scheme the rate change instants of the VBR source will be estimated and the feedbacks will be generated in advance ($2T_d$ before the estimated VBR rate changes occur).

Let X_k denote the length of the time interval over which the VBR source maintains a constant rate. That is, $X_k = t_k - t_{k-1}$. Let $\hat{X}$ denote an estimator for X_k. Under the *PF* scheme the transmission instant of the feedback depends on t_k, X_k, $\hat{X}$ and the roundtrip propagation delay $2T_d$. Let f_k denote the time instant at which the k^{th} feedback is transmitted. If $X_k > \hat{X} - 2T_d$, the network access node transmits the feedback to the ABR source at time $t_{k-1} + \hat{X} - 2T_d$. If $X_k < \hat{X} - 2T_d$, the feedback is transmitted at $t_{k-1} + X_k$ as under the *NPF* scheme. Therefore,

$$f_k = t_{k-1} + min\{X_k, \hat{X} - 2T_d\}$$

Figure 5 illustrates an example of feedback transmission instants. Since X_{k-1} and X_{k+1} is greater than $\hat{X} - 2T_d$, the feedbacks corresponding to these intervals are generated at $t_{k-2} + \hat{X} - 2T_d$ and $t_k + \hat{X} - 2T_d$. As $X_k < \hat{X} - 2T_d$, the feedback corresponding to this interval is generated at time $t_{k-1} + X_k$.

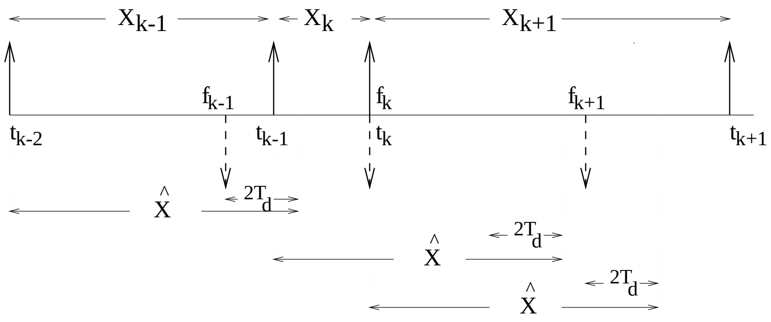

Figure 5: A realization of feedback transmission instants

Note that, because of the roundtrip propagation delay, the adjusted ABR rate reaches the network access node at $f_k + 2T_d$.

In order to compare the effectiveness of the *PF* scheme with *NPF* scheme described in the previous section, the magnitude of the induced bandwidth mismatches for both schemes can be considered. Since the ABR cell losses are caused by the overutilization periods captured by the bandwidth mismatch, the expected bandwidth mismatch would reflect the efficiency of a feedback based flow control scheme in terms of the induced cell losses.

As described before, the feedback is transmitted when a VBR rate change is detected under the *NPF* scheme. Thus, the induced bandwidth mismatch is always equal to the roundtrip propagation delay, $2T_d$. Thus, the expected value of the amount of induced bandwidth mismatch is $2T_d$. Let C_{NPF} be equal to this amount, thus $C_{NPF} = 2T_d$.

Let C_{PF} be the expected value of the amount of bandwidth mismatch induced and W_{PF} be a random variable indicating the amount of bandwidth mismatch under the *PF* scheme. Thus, $C_{PF} = E\{W_{PF}\}$. Under the proposed *PF* scheme W_{PF} is equal to,

$$\begin{aligned} W_{PF} &= |t_k - (f_k + 2T_d)| \\ &= |X_k - min\{X_k, \hat{X} - 2T_d\} - 2T_d| \end{aligned}$$

$$= \begin{cases} 2T_d & \text{if } X_k \le \hat{X} - 2T_d \\ \hat{X} - X_k & \text{if } \hat{X} - 2T_d + 1 \le X_k < \hat{X} \\ 0 & \text{if } X_k = \hat{X} \\ X_k - \hat{X} & \text{if } X_k > \hat{X} \end{cases}$$

Let $f(X_k)$ denote the distribution of X_k (the VBR time scale). An example distribution is shown in Figure 6. Let $\hat{X}$ be the estimate of X_k.

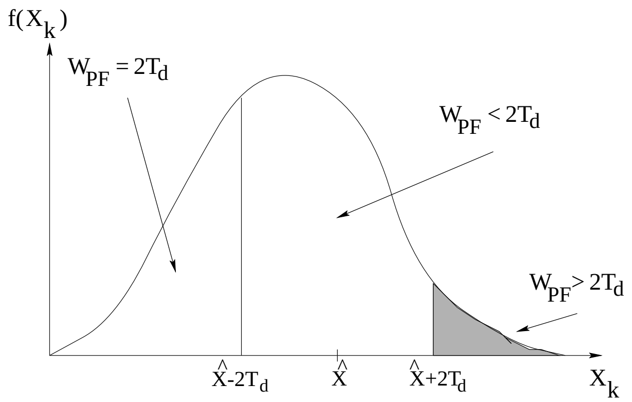

Figure 6: An example distribution of X_k

If X_k is in the region $1 \le X_k \le \hat{X} + 2T_d$, then the bandwidth mismatch is always equal to or less than the roundtrip propagation delay. Therefore, in this region $W_{PF} \le W_{NPF} = 2T_d$. The only region in which the *PF* scheme may lead to more bandwidth mismatch than the *NPF* scheme is $X_k > \hat{X} + 2T_d$, since only in this region the bandwidth mismatch is greater than the roundtrip propagation delay. Therefore, the effectiveness of the *PF* scheme depends on the tail of the distribution of X_k. If the estimator chosen can decrease the probability of entering into this region while increasing the probability of entering into the low bandwidth mismatch region the effectiveness of the *PF* scheme can be increased.

Claim : If the maximum value that X_k can achieve is finite, a value of $\hat{X}$ (estimator for the *PF* Scheme) can always be found such that the *PF* scheme is at least as good as the *NPF* scheme, $C_{PF} \le C_{NPF}$.

Proof: Let X_{max} denote the maximum value of X_k. Since a bandwidth mismatch larger than $2T_d$ may occur only in the region $X_k > \hat{X} + 2T_d$, $\hat{X}$ can be chosen such that $\hat{X} + 2T_d \ge X_{max}$. Therefore, $X_k > \hat{X} + 2T_d \ge X_{max}$ will never occur and the bandwidth mismatch will never exceed $2T_d$. Since for $X_k \le \hat{X} + 2T_d$, bandwidth mismatch is less than or equal to $2T_d$, $C_{PF} \le C_{NPF} = 2T_d$.

5 Numerical Results

5.1 The Impact of Time Scales on the Feedback Based Flow Control Schemes

In this subsection, the impact of various time scales (network, ABR and VBR) on the effectiveness of the *NPF* scheme is investigated by using the ABR cell loss probability derived in Section 3.

Figure 7 illustrates the ABR cell loss probability as a function of p_f for $p_s(0) = p_s(1) = p_s = 0.005, 0.001, 0.0005$ and 0.0001. For this plot, the results are derived for VBR source rates $r_v(1) = 0.8$ and $r_v(0) = 0.4$ cells/slot and a buffer with capacity 40. As the propagation delay decreases (p_f increases), the amount of time that it takes for the ABR source to respond to the feedbacks generated at the network access node decreases. As a consequence, the amount of bandwidth mismatch (thus the overutilization periods) decreases, causing a decrease in the ABR cell loss probability. In addition to the propagation delay, the VBR time scale ($1/p_s$) also has a considerable effect on the ABR cell loss probability. When the VBR time scale decreases (p_s increases), VBR source rate changes occur more frequently. Therefore, more bandwidth mismatch cycles are initiated resulting in more ABR cell losses. Note that, $p_s \ll p_f$ in order for the assumption of no multiple pending feedbacks to be reasonably accurate.

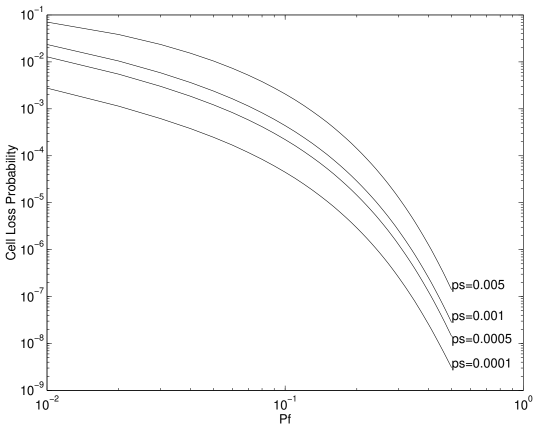

Figure 7: ABR cell loss probability vs. p_f for various p_s

Figures 8 and 9, illustrate the ABR cell loss probability as a function of batch size B_k for buffer capacities of $10, 15, 20, 25$ and 30. The distance between the ABR source and the network access node is assumed to be 20000 and 200 slots for Figure 8 and Figure 9 respectively. Since the VBR source rates are assumed to be $r_v(1) = 0.8$ and $r_v(0) = 0.4$, the fundamental subframe lengths are 2 and 6 slots. Thus, a B_k-order subframe (ABR time scale) has lengths of $2B_k$ and $6B_k$ slots. For a fixed value of buffer capacity, it can be observed that the ABR cell loss probability initially decreases as B_k (the ABR time scale) increases. This behavior is reversed when B_k exceeds a threshold. Thus, for a given buffer capacity, there is an optimal B_k (or ABR time scale) that minimizes the induced ABR cell losses. The optimal B_k also depends on the propagation delay. For example, the optimal B_k for a buffer capacity of 15 is equal to 8 in Figure 8 while it is equal to 2 in Figure 9. This trend may be attributed to the decreasing positive impact of a large ABR time scale for a decreased propagation delay.

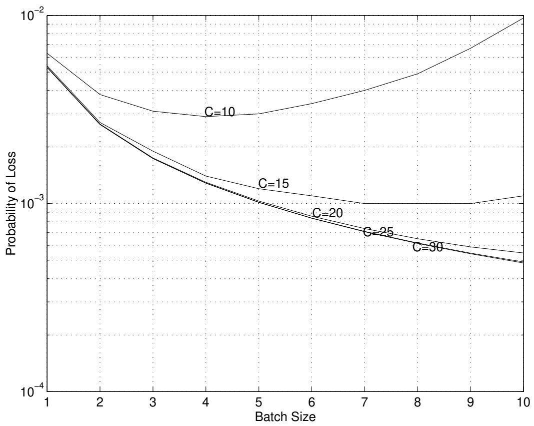

Figure 8: ABR cell loss probability vs. B_k for various values of C for an average distance of 20000 slots

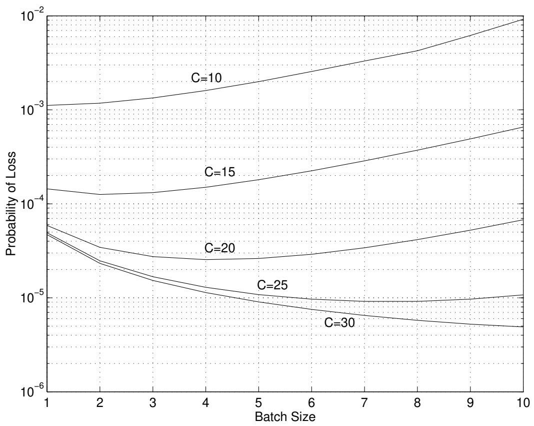

Figure 9: ABR cell loss probability vs. B_k for various values of C for an average distance of 200 slots

5.2 The ABR Cell Loss Probability under the *PF* Scheme

In this subsection, in order to illustrate the effectiveness of the *PF* scheme with respect to the *NPF* scheme, the expected amount of bandwidth mismatch is calculated for both schemes and some simulation results are presented in terms of loss probabilities. For this section, it is assumed that the maximum length for X_k is 100 slots.

Figure 10 shows the expected amount of bandwidth mismatch for the *PF* and the *NPF* schemes when X_k has a binomial distribution with parameters 100 and 0.5, thus $X_k \sim Bin(100, 0.5)$. For this distribution, it turns out that the C_{PF} reaches its minimum when $\hat{X} = 50$ (the mean of the binomial distribution).

Since the overutilization periods of the bandwidth mismatch may induce cell losses, a similar effect is expected in terms of cell losses. To illustrate this, some simulation results are presented next. For the simulations the following values are assumed. The buffer at the network access node has a capacity of 30. The VBR source rates are $r_v(1) = 0.8$ and $r_v(0) = 0.4$ cells/slot and the

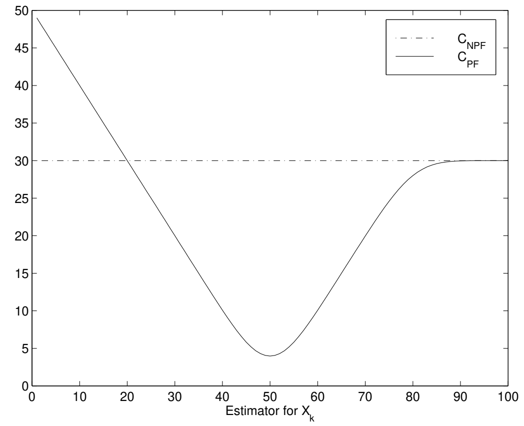

Figure 10: Comparison of C_{NPF} and C_{PF} for $X_k \sim Bin(100, 0.5)$

corresponding ABR source rates are 0.167 and 0.5 cells/slot.

In Figure 11, the ABR cell loss probabilities for the *PF* scheme and *NPF* schemes are plotted as a function of the estimate $\hat{X}$ for $2T_d = 20$ and $2T_d = 30$. As expected, the best estimator for X_k is around the mean of the distribution. Once a good estimator for X_k is chosen, there is a significant gain in terms of losses. If $\hat{X}$ is close to X_{max}, the loss probabilities under the *PF* scheme converge to those induced by the *NPF* schemes, since in this case feedback is transmitted mostly at the instants of rate changes (as opposed to earlier). Also, the effects of different propagation delays looks very similar under the *PF* scheme when the chosen estimator is good. Because, with a good estimator the *PF* scheme is almost independent of the propagation delay.

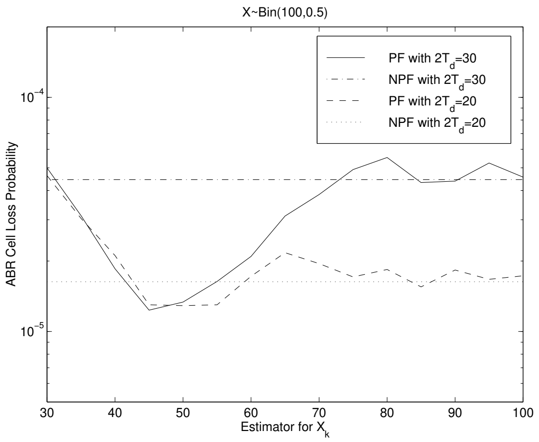

Figure 11: ABR Cell Loss Probability vs. $\hat{X}$

6 Conclusions

In this paper, the impact of network, VBR and ABR time scales on the effectiveness of feedback based flow control schemes is studied and a proactive feedback based flow control scheme which tries to reduce the amount of bandwidth mismatch is introduced.

The network time scale is defined as the transmission time of a cell. The VBR time scale is defined as the average time period over which the VBR application maintains a constant rate and the ABR time scale is defined as the distance between consecutive blocks of consecutive cells generated by the ABR source.

Since the decreased network time scale corresponds to the increased propagation delay, increased network time scale increases the effectiveness of feedback based flow control schemes. The increased VBR time scale has also a positive impact on the effectiveness of feedback based flow control schemes. This is due to the fact that, less frequent rate changes occur when the VBR time scale increases. The ABR time scale may have a positive impact as well. It is observed that, increased ABR time scale initially decreases the ABR cell loss probability, reaching a minimum at a threshold and then the situation is reversed. The threshold where the ABR cell loss probability reaches its minimum value also depends on the propagation distance. For the increased propagation delay, the threshold tends to be larger. Thus the impact of all time scales should be considered to accurately evaluate the effectiveness of a feedback based flow control scheme.

Under the above scheme (*NPF*) the network access node transmits the feedbacks to the ABR source when it detects rate changes at the network node. Thus, a bandwidth mismatch which is equal to the roundtrip propagation delay is unavoidable. But, the bandwidth mismatch can be reduced if the exact time instants of VBR source rate changes are known or estimated suitably. By transmitting the feedbacks a roundtrip propagation delay before the estimated rate changes, the amount of bandwidth mismatch can be reduced which also reduces the induced ABR cell losses. This scheme which is referred as the *PF* scheme guarantees to be at least as good as the *NPF* scheme by choosing a suitable estimator for the VBR source rate change instants.

References

[1] ATM Forum, "Traffic Management Specification Version 4.0", *ATM Forum/95-0013R10*, Feb. 1995.

[2] F. Bonomi and R. Morris, "The Rate Based Flow Control Framework for the Available Bit Rate ATM Service", *IEEE Network*, pp. 25-39, Mar./Apr. 1995.

[3] J. C. Bolet and A. Shankar, "Dynamical Behavior of Rate Based Flow Control Mechanism", *ACM Comp. Commun Rev.*, pp. 35-49, Apr. 1990.

[4] S. Liu et al., "Fairness in Closed Loop Rate Based Traffic Control Schemes", *ATM Forum/94-0387*, May 1994.

[5] H. T. Kung and R. Morris, "Credit Based Flow Control for ATM Networks", *IEEE Network*, pp. 40-48, Mar./Apr. 1995.

[6] H. T. Kung and K. Chang, "Receiver-Oriented Adaptive Buffer Allocation in Credit-Based Flow Control for ATM Networks," *INFOCOM'95*, pp. 239-252, 1995.

[7] J. F. Ren and J. W. Mark, "Design and Analysis of a Credit Based Controller for Congestion Control in B-ISDN/ATM Networks," *INFOCOM'95*, pp. 40-48, 1995.

[8] K. K. Ramakrishnan and P. Newman, "Integration of Rate Based and Credit Schemes for ATM Flow Control", *IEEE Network*, pp. 49-56, Mar./Apr. 1995.

[9] N. Yin and M. G. Hluchjy, "On Closed-Loop Rate Control for ATM Cell Relay Networks," *INFOCOM'94*, pp.99-108, Toronto, 1994.

[10] R. Beraldi and S. Morano, "Selective BECN Schemes for Congestion Control of ABR traffic in ATM LAN," *ICC'96*, pp. 503-507, 1996.

[11] A. Barnhart, "Baseline Performance Using PRCA Rate Control," *ATM Forum/94-0597*, July 1994.

[12] A. Charny et al., "Congestion Control with Explicit Rate Indications," *ICC'95*, pp. 1954-1963, Seattle, 1995.

[13] L. Roberts, "Enhanced PRCA," *ATM Forum/94-0735R1*, Aug. 1994.

[14] Y. T. Wang and B. Sengupta, "Performance Analysis of a Feedback Congestion Control Policy Under non-negligible Propagation Delay," *ACM SIGCOMM'91*, pp. 149-157, Sep. 1991.

[15] M. Abdelaziz and I. Stavrakakis, "Study of an Adaptive Rate Control Scheme Under Unequal Propagation Delays," *ICC'95*, pp.1964-1968, Seattle, 1995.

[16] R. Pazhyannur and R. Agrawal, "Feedback Based Flow Control in ATM Networks with Multiple Propagation Delays," *1996 IEEE*, pp. 585-93.

[17] T. Dag and I.Stavrakakis, "Study of the Impact of Network and Source Time Scales on Feedback Based Congestion Control," *SPIE'96*, Nov. 1996.

7 Appendix

7.1 Calculation of the $P(s_k j_k; s_{k+1} j_{k+1})$

Let $(s_k j_k) \rightarrow (s_{k+1} j_{k+1})$ denote a state transition from state (s_k, j_k) to state (s_{k+1}, j_{k+1}). Notice that for some values of s_k and j_k the state transitions are not possible or they occur with very low probabilities (can be approximated that they never occur).

Let the current VBR state, s_k, and the feedback state ,j_k, be equal to 0. If the VBR rate changes at t_{k+1}, a feedback will be generated for the ABR source so that it would adjust its rate to the new VBR rate. Therefore, a $(00) \rightarrow (10)$ transition is impossible (as the feedback is not generated), that is $P(00; 10) = 0$. In this case, the only transition is $(00) \rightarrow (11)$ denoting that the VBR rate is increased and a feedback is generated. This transition has a probability $P(00; 11) = p_s(0)$ where $p_s(0)$ is the probability that S_k changes state at the end of the k^{th} subframe at the beginning of which it was in state $s_k = 0$. A state transition $(00) \rightarrow (01)$ is also impossible because a feedback cannot be generated unless there is a change in the VBR state. Thus $P(00; 01) = 0$.

With similar arguments all other state transition probabilities can be calculated easily. The state diagram for the $\{S_k, J_k\}$ process is shown in Figure 12.

7.2 Calculation of $P(q_{k+1}/s_k j_k q_k)$

In order to determine the evolution of the Markov chain, the transition probability $P(q_{k+1}/s_k j_k q_k)$ needs to be determined. In this subsection the derivation of $P(q_{k+1}/s_k j_k q_k)$ is shown using the one slot transition probabilities.

As shown in Figure 13, an ABR cell arrival always occurs in the first B_k subsequent slots of the subframe with length $B_k T_k$. Although the ABR cell arrivals are limited to the first B_k

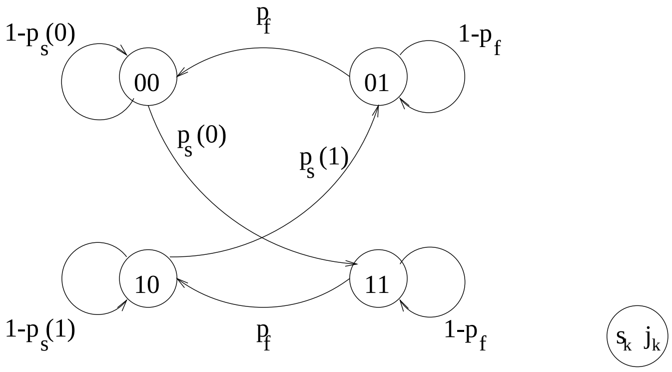

Figure 12: The state diagram of the $\{S_k, J_k\}$ process

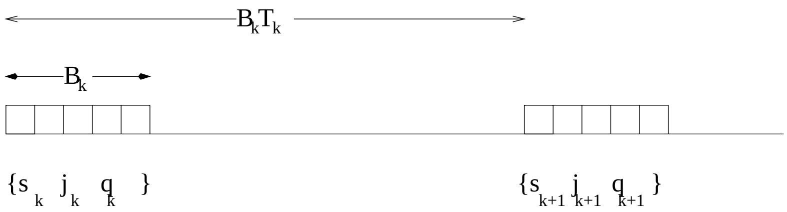

Figure 13: ABR cell arrival process

slots of each subframe, a VBR cell arrival may occur anywhere in the subframe. Therefore, each subframe can be divided into two parts and be examined separately to facilitate the evaluation of $P(q_{k+1}/s_k j_k q_k)$. The first part consists of the first B_k slots over which there are arrivals from both sources; the second part consists of the remaining $B_k T_k - B_k$ slots over which there are arrivals only from the VBR source.

Let $q_{k,i}$ denote the queue occupancy at the end of the i^{th} slot of the k^{th} subframe and $P_A(q_{k,i+1}/s_k j_k q_{k,i})$ and $P_B(q_{k,i+1}/s_k j_k q_{k,i})$ denote the one slot transition probabilities from $q_{k,i}$ to $q_{k,i+1}$ over the first part of the subframe (or first B_k slots) and the second part of the subframe (or the last $B_k T_k - B_k$ slots), respectively. The derivation of these probabilities are shown in detail in the following subsections.

7.2.1 One Slot Transition Probability with Arrivals from Both Sources

The one slot transition probability $P_A(q_{k,i+1}/s_k j_k q_{k,i})$ can be calculated as follows for $1 \le i \le B_k$. For $q_{k,i} = 0$, $0 \le q_{k,i+1} \le C - 1$:

$q_{k,i+1} = A(s_k) + 1$ where $A(s_k)$ denotes the number of arrivals from the VBR traffic source in one slot when the current VBR state is s_k. In this equation, 1 accounts for the guaranteed ABR cell arrival. Since, the initial buffer occupancy $q_{k,i}$ is equal to 0 and cell arrivals are assumed to occur after cell departures no service is provided. Therefore,

$$P_A(q_{k,i+1}/s_k j_k q_{k,i}) = P\{A(s_k) = q_{k,i+1} - 1\}$$

For $1 \le q_{k,i} \le C$, $0 \le q_{k,i+1} \le C - 1$:

In this case $q_{k,i+1} = q_{k,i} + A(s_k)$. Since the buffer is nonempty at $q_{k,i}$, one cell is served and $A(s_k) + 1$ cells arrive, resulting in a buffer occupancy of $q_{k,i+1} = q_{k,i} + A(s_k) + 1 - 1 = q_{k,i} + A(s_k)$ at the beginning of the next slot $q_{k,i+1}$. Thus,

$$P_A(q_{k,i+1}/s_k j_k q_{k,i}) = P\{A(s_k) = q_{k,i+1} - q_{k,i}\}$$

For $0 \leq q_{k,i} \leq C$, $q_{k,i+1} = C$:

Since the buffer occupancy at $q_{k,i+1}$ is C, some cells may be lost. $C = q_{k,i} + A(s_k)$. If the number of VBR cell arrivals is greater than $C - q_{k,i}$, $A(s_k) - C + q_{k,i}$ cells will be lost. Therefore,

$$P_A(q_{k,i+1} = C/s_k j_k q_{k,i}) = \sum_{m=0}^{1-C+q_{k,i}} P\{A(s_k) = C - q_{k,i} + m\}$$

7.2.2 One Slot Transition Probability with Arrivals from VBR Source

In this case there may only be arrivals from the VBR source. The one slot transition probability $P_B(q_{k,i+1}/s_k j_k q_{k,i})$ can be calculated in a similar way as $P_A(q_{k,i+1}/s_k j_k q_{k,i})$. The only difference is that the total number of cell arrivals per slot is one less compared to the previous case.

For $q_{k,i} = 0$, $0 \leq q_{k,i+1} \leq C$:

As the initial buffer occupancy is equal to 0, no cells can be served and since only VBR cell arrivals are possible, $q_{k,i+1} = A(s_k)$; thus,

$$P_B(q_{k,i+1}/s_k j_k q_{k,i}) = P\{A(s_k) = q_{k,i+1}\}$$

For $1 \leq q_{k,i} \leq C$, $0 \leq q_{k,i+1} \leq C$:

In this case $q_{k,i+1} = q_{k,i} + A(s_k) - 1$ where -1 accounts for the served cell. Therefore,

$$P_B(q_{k,i+1}/s_k j_k q_{k,i}) = P\{A(s_k) = q_{k,i+1} - q_{k,i} + 1\}$$

7.2.3 The $B_k T_k$ Slot Transition Probability $P(q_{k+1}/s_k j_k q_k)$

Using the probabilities calculated in the previous subsections, the $B_k T_k$ slot transition probability can be determined. The $B_k T_k$ slot transition probability $P(q_{k+1}/s_k j_k q_k)$ describes the probability that the queue occupancy at the beginning of the next subframe is equal to q_{k+1} given the current subframe parameters s_k, j_k and q_k.

Using recursion, the transition probability for the first part of the subframe and for the second part of the subframe can be calculated as shown below. For the B_k slot transition probability $P_A(q_{k,B_k}/s_k j_k q_k)$, $B_k - 1$ and 1 slot transition probabilities are needed. Thus,

$$P_A(q_{k,B_k}/s_k j_k q_k) = \sum_{q_{k,B_k-1}=0}^{C} P_A(q_{k,B_k-1}/s_k j_k q_k) P_A(q_{k,B_k}/s_k j_k q_{k,B_k-1})$$

Similarly, the $B_k T_k - B_k$ slot transition probability $P_B(q_{k+1}/s_k j_k q_{k,B_k})$ can be calculated and is given by,

$$P_B(q_{k+1}/s_k j_k q_{k,B_k}) = \sum_{q_{k,B_k T_k-1}=0}^{C} P_B(q_{k,B_k T_k-1}/s_k j_k q_{k,B_k}) P_B(q_{k+1}/s_k j_k q_{k,B_k T_k-1})$$

Combining these two equations $P(q_{k+1}/s_k j_k q_k)$ is calculated as follows.

$$P(q_{k+1}/s_k j_k q_k) = \sum_{q_{k,B_k}=0}^{C} P_A(q_{k,B_k}/s_k j_k q_k) P_B(q_{k+1}/s_k j_k q_{k,B_k})$$

7.3 Calculation of the ABR Cell Loss Probability

Let $I(s_k, j_k, q_k; i)$ $(R(s_k, j_k, q_k; i))$ denote the number of cells lost (arrived) at the i^{th} slot of the k^{th} subframe in state (s_k, j_k, q_k); $1 \leq i \leq B_k T_k$. Clearly, $R(s_k, j_k, q_k; i)$ does not depend on the queue occupancy and is only a function of s_k, j_k and i. Thus,

$$R(s_k, j_k; i) = \begin{cases} A(s_k) & \text{if } i > B_k \\ A(s_k) + 1 & \text{if } i \leq B_k \end{cases}$$

where $A(s_k)$ denotes the number of VBR cell arrivals in a slot when the current VBR state is s_k.

The number of lost cells in a slot can be found by considering the number of arrivals in the slot, the buffer occupancy in the previous slot and the buffer capacity C. Therefore,

$$I(s_k, j_k, q_k; i) = \begin{cases} m & \text{if } R(s_k, j_k; i) = C + 1 - q_{k,i-1} + m \\ 0 & \text{otherwise} \end{cases}$$

where $q_{k,i-1}$ denotes the queue occupancy at the $i - 1^{th}$ slot of the k^{th} subframe.

Clearly, the number of cell arrivals over the subframe starting with system Markov Process $\{S_k, J_k, Q_k\}_{k \geq 1}$ in state (s_k, j_k, q_k) is the summation of $R(s_k, j_k; i)$ for all slots. Thus, the average number of cell arrivals in a subframe $\{S_k, J_k, Q_k\}_{k \geq 1}$ in state (s_k, j_k, q_k) can be expressed as,

$$\begin{aligned} \overline{M}(s_k, j_k, q_k) &= \sum_{i=1}^{B_k T_k} E\{R(s_k, j_k, q_k)\} \\ &= B_k + B_k T_k r_v(s_k). \end{aligned}$$

The total number of cells lost over the entire subframe is equal to the summation of the $I(s_k, j_k, q_k; i)$ for all i slots of the subframe. Thus, for $\overline{L}(s_k, j_k, q_k)$ the following equation is obtained.

$$\overline{L}(s_k, j_k, q_k) = \sum_{i=1}^{B_k T_k} E\{I(s_k, j_k, q_k; i)\}$$

After some manipulations, $\overline{L}(s_k, j_k, q_k)$ can be shown to be equal to,

$$\begin{aligned} \overline{L}(s_k, j_k, q_k) &= \sum_{i=1}^{B_k} \sum_{l=0}^{C} \sum_{m=0}^{l-C+1} m P\{A(s_k) = C - l + m / q_k, s_k, j_k\} \\ &\times \; P\{q_{k,i-1} = l / q_{k,0} = q_k\} \end{aligned}$$

Combining $\overline{L}(s_k, j_k, q_k)$ and $\overline{M}(s_k, j_k, q_k)$ the ABR cell loss probability can be expressed as follows.

$$\begin{aligned} LP &= \sum_{s_k=0}^{1} \sum_{j_k=0}^{1} \sum_{q_k=0}^{C} \frac{\Pi(s_k, j_k, q_k)}{B_k + r_v(s_k) B_k T_k} \\ &\times \sum_{i=1}^{B_k} \sum_{l=0}^{C} \sum_{m=0}^{l-C+1} m P\{A(s_k) = C - l + m / q_k, s_k, j_k\} \\ &\times \; P\{q_{k,i-1} = l / q_{k,0} = q_k\} \end{aligned}$$